



Experimental Study of Mixed Convection in an Enclosure with a Cold Movable Top Wall and Hot Bottom Wall

Nabil J. Yasin*

Dhia Al-Deen H. Alwan**

Ayad S. Abdulla***

*,** Department of Airconditioning and Refrigeration Engineering / Engineering Technical College of Baghdad

*** Department of Airconditioning and Refrigeration Engineering / Engineering Technical College of Mosul

*Email: nabiljamil58@yahoo.com

**Email: dhia716@yahoo.com

***Email: ayad_s00@yahoo.com

(Received 4 November 2013; accepted 28 January 2014)

Abstract

Mixed convection heat transfer to air inside an enclosure is investigated experimentally. The bottom wall of the enclosure is maintained at higher temperature than that of the top wall which keeps in oscillation motion, whereas the left and right walls are well insulated. The differential temperature of the bottom and top walls changed several times in order to accurately characterize the temperature distribution over a considerable range of Richardson number. Adjustable aspect ratio box was built as a test rig to determine the effects of Richardson number and aspect ratio on the flow behavior of the air inside the enclosure. The flow fields and the average Nusselt number profiles were presented in this work. The results show that, at a constant value of the Richardson number, average Nusselt number (Nu_{av}) increases with aspect ratio. Furthermore, as Richardson number decreases, the time period decreases with constant values of aspect ratio.

Keywords: *Mixed convection, Experimental, Aspect ratio, Enclosure, Oscillating motion.*

1. Introduction

The problem of heat transfer by mixed convection has been the subject of intensive numerical, and experimental investigations in the recent years because of its significant applications in nature and in many scientific and engineering practices such as, cooling of electronic devices[1], the design stage of Ceiling Radiant Cooling Panel (CRCP) system [2], manufacturing of solar collectors, flow and heat transfer in solar ponds[3]. A survey of the literature on mixed convection in enclosures shows that most of these studies were adapted the numerical methods while very few of these studies were carried out experimentally. Aydin, and Yang [4] investigated numerically mixed convection in cavities with a locally heated lower wall and moving sidewalls which was assumed to be moving downward

across the cavity and to be kept at a constant temperature. The remaining parts of the cavity were considered to be adiabatic. Mixed convection heat transfer in a two-dimensional rectangular cavity with constant heat flux from partially heated bottom wall while the isothermal sidewalls were moving in the vertical direction, was studied by Guo and Sharif [5]. All computations were done for a range of Richardson number from (0.1 to 10). The results show an improvement of the flow and temperature field and increasing of the Nusselt number values by increasing of both of the Richardson number and the heat source. Hakan and Dagekin[6], Abdalla Al-Amiri, et al.[7], Sharif [8], and Waheed, [9] were also studied the problem for the mixed convection in enclosures under different boundary conditions numerically and they concluded a number of explanations for the change in the

values of the Nusselt number. Khanafer and Amiri[10] investigated the effects of oscillatory motion of the upper wall. The results reveal that the Reynolds and Grashof numbers would either enhance or retard the energy transport process and drag force behavior depending on the velocity cycle. Ghasemi, and Aminossadat[11] present a numerical investigation of mixed convection in a square cavity which configured such that one of the vertical walls is cooled and slides either with a constant speed or with a sinusoidal oscillation. The results indicate that the direction and magnitude of the sliding wall velocity affect the heat transfer rate. An experimental study of mixed convection and flow pattern in a lid-driven arc-shape cavity were carried out by Chen and Cheng[12]. The top flat lid maintained at temperature ΔT_L and was moving from left to right at a constant speed. The bottom arc-shape wall is heated such that its temperature is fixed at a higher temperature. The flow visualization technique using kerosene smoke is applied to observe the flow pattern. An experimental investigation for the flow field in an enclosure with a bottom wall maintained at a temperature higher than the temperature of the top wall was done in the present work. The top wall was moving horizontally in a certain sinusoidal motion while the two other walls were perfectly insulated. The air was used to be the working fluid.

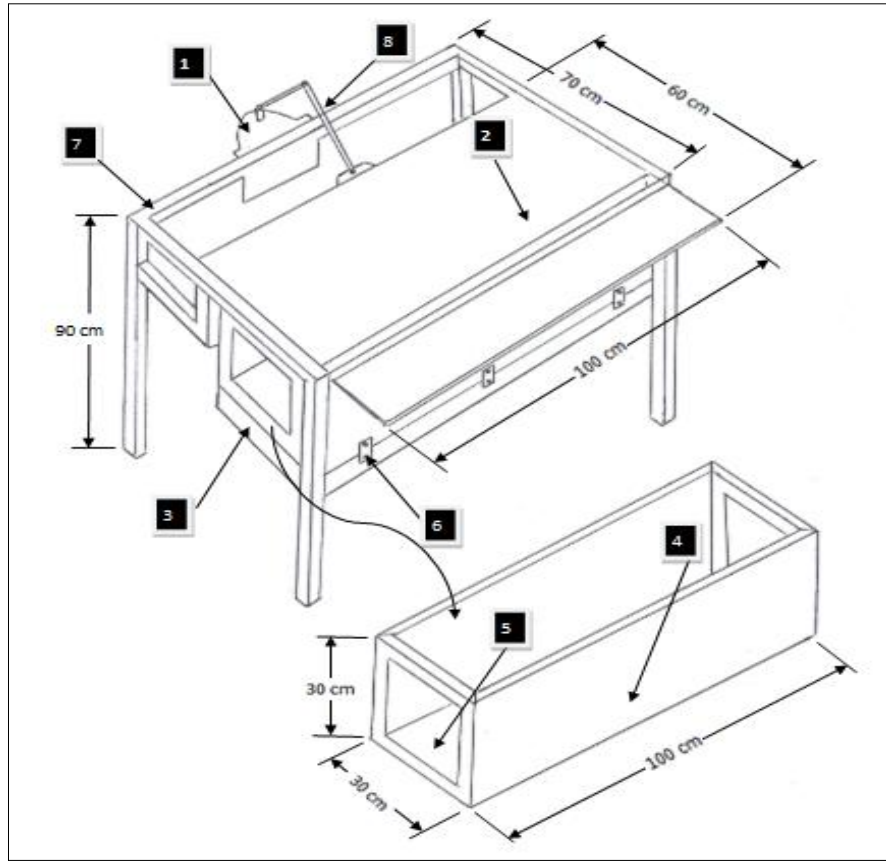
2. Experimental Apparatus and Procedure

The schematic diagram of the test rig is shown in Fig.(1). The main part of the experimental rig is the enclosure which shown in Fig. (2). It is a rectangular box manufactured from wood. The enclosure has a width of (300) mm and a variable height of (150)mm, (300)mm, and (600) mm. To ensure that the flow is two-dimension, the depth of the enclosure is adjusted to (1000) mm[13]. The bottom wall is heated by an external plate heater fixed by bolts. Three holes on the bottom side used to inject smoke inside the enclosure as shown in Fig.(3). The top wall is connected to an external mechanism to provide an oscillating motion. The moving apparatus was designed and fabricated to provide a horizontal variable speed motion to the top wall according to $[u = u_{\max} \sin(\omega t)]$. The oscillation amplitude (u_{\max}) represent the maximum top wall moving speed as shown in Fig. (4). Fig. (5) shows the moving apparatus which consists of (600mm x 1000 mm) aluminum plate, (3 mm) thickness connecting to a variable speed DC-motor with an arm. A slice of

rubber was inserted between the movable part (aluminum plate) and the sides of the enclosure to prevent air leakage. The left and right walls of the enclosure were perfectly insulated to ensure that no heat exchange across them. The symptomatic walls of the enclosure provided with two glass windows to visualize the flow field inside the enclosure as shown in Fig.(6). An electrical film heater was mounted on the bottom surface of the enclosure to provide a constant heat flux. Many strips of Chrome-Nickel alloy having a width of (1) mm and of (48) ohm/m electrical resistance used as heating element. The heating element supplied a wide range of constant heat flux values. The power required for the heating element was controlled by adjusting the electric current supplied to the element. The flow field was visualized by imaging the smoke inside the enclosure. Type-K thermocouples with a digital thermometer were used to measure the temperature distribution inside the enclosure, and the differential temperature of the cold and hot sides as in Fig.(7). The thermocouples were connected in parallel to a digital thermometer by leads through a selector switch. In order to obtain accurate measurements, a calibration for the thermocouples, compensating cable, selector switch, and the measuring device were done. The angular velocity of the motor is measured by using speed meter. Air flow visualized using smoke method technique. The smoke is fed into the cavity through three holes placed beneath the bottom wall of the enclosure. The two glass windows and the smoke allowed the flow field in the enclosure to be visualized by using a digital camera. During each test run, the temperature of the bottom heating surface and the top moving wall is specified and the accessories is setting according to these selected specification. A digital watch was used to control the time period of oscillation. The temperatures of the hot and the cold walls were monitoring continuously (three thermocouples T_1 , T_2 , and T_3 for the hot wall, and one thermocouple T_7 for the cold wall) as in Fig (7). Each (1/4) and (3/4) period, the air temperature inside the enclosure was recorded. When the recorded temperature of a previous period and that of the later period is almost equal, for the entire air in the enclosure, the experiment assumed to be reached the steady state condition. When the enclosure is considered to be at a steady state condition the smoke has been injected to the cavity through the three holes of the bottom wall and photographs of the flow field have been done by using the digital camera. At the end of the experiment, the heating element switch off, and

the rig will allowed returning to its original temperature before starting new test run. The analyses of the experimental uncertainties of the results have been given proper attention. In the present study, the uncertainty analysis was

performed by the method proposed by Holman 1984[14] for all experiments, and it was found that the expected experimental error was within $\pm 4.3\%$ for all test runs.



- | | |
|------------------------------|---------------------|
| 1. DC motor | 5. Glass window |
| 2. Aluminum plate 5 mm thick | 6. Joint with screw |
| 3. Electrical heater | 7. Iron frame |
| 4. Wood Enclosure | 8. Flexible arm |



Fig. 1. Schematic diagram and a photograph of the test rig.

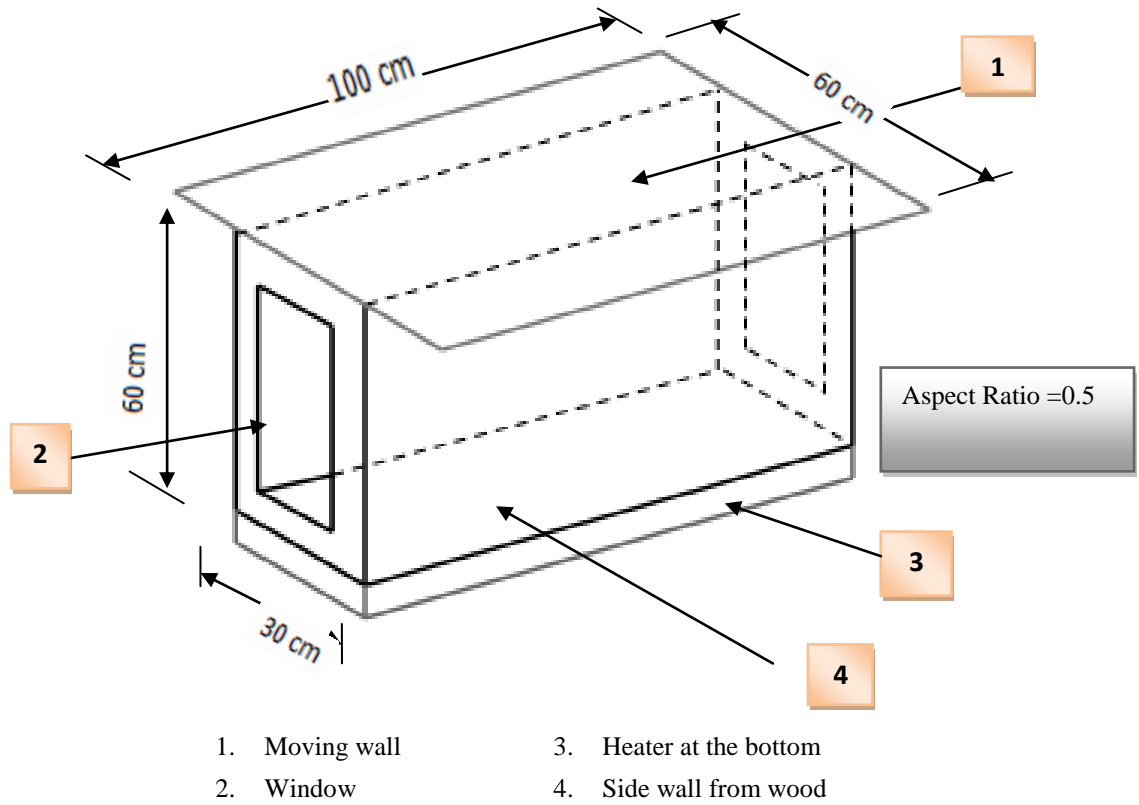


Fig. 2. Schematic diagram of the enclosure.

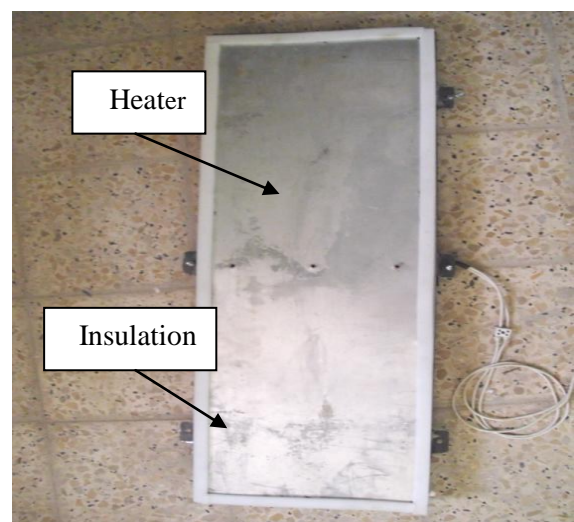
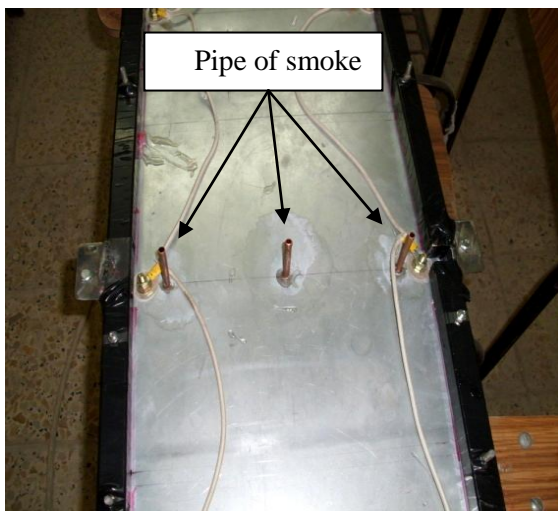


Fig. 3. The bottom wall.

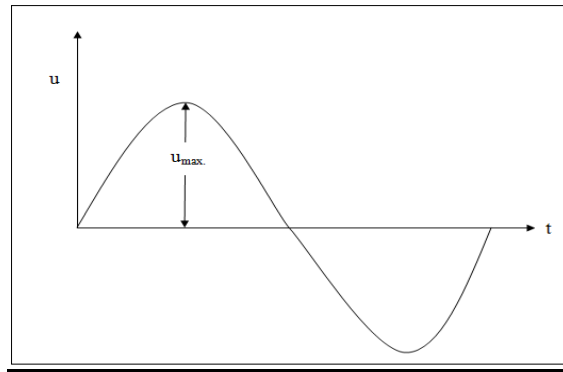


Fig. 4.The amplitude of oscillation.

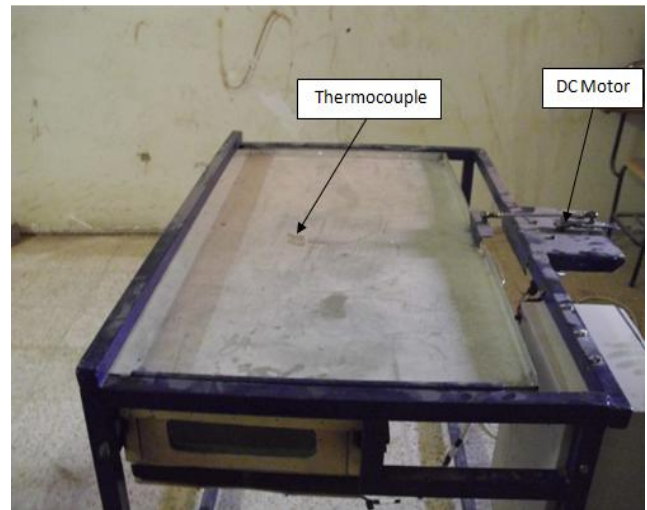
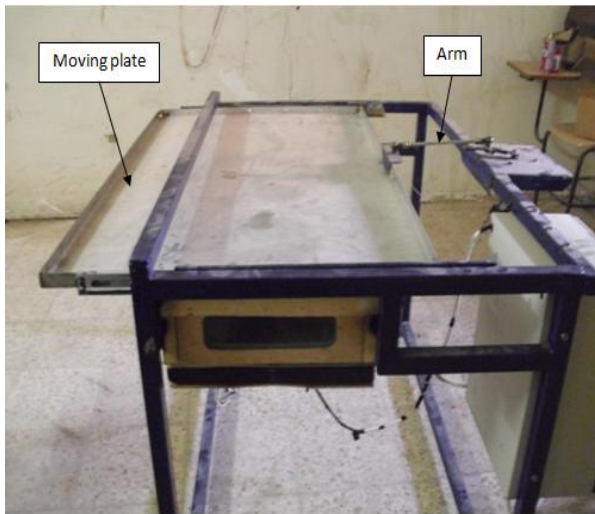


Fig. 5.The movable top wall.

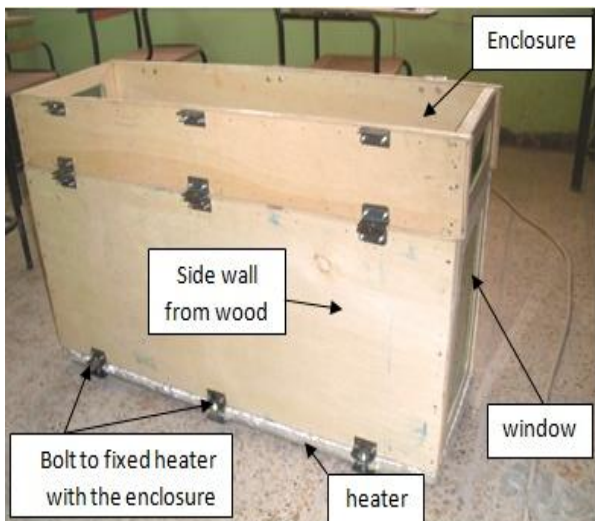


Fig. 6.The side wall of enclosure.

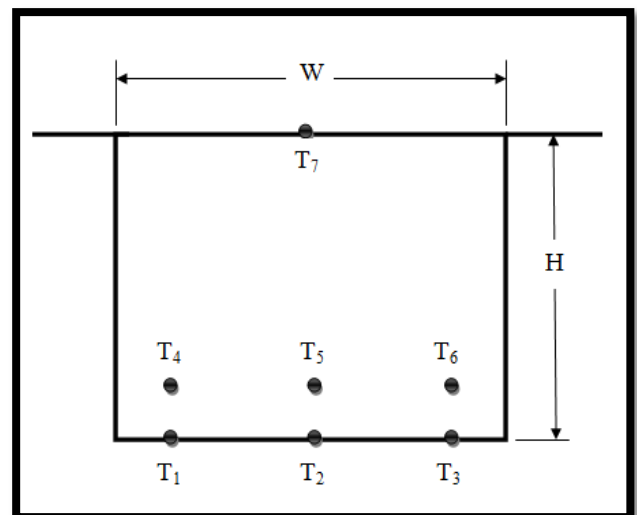


Fig. 7. Thermocouple distribution inside the enclosure.

3. Data Analysis

Richardson number is a measurement of the relative importance variables of the buoyancy-driven natural convection to the lid-driven forced convection, which is calculated from the following equation.

$$Ri = Gr/Re^2 = (g \cdot \beta \cdot (T_h - T_c) \cdot H) / (u_{max})^2 \quad \dots(1)$$

where

$$u_{max} = \omega \cdot r$$

The Nusselt number is assumed to be the reference to the effect of fluid motion on heat transfer. It is of a great interest to study this effect by determining Nusselt number in each stage of heat transfer process within the enclosure. Generally, and according to the heat balance which occurs between the heating surface and the air inside the enclosure, one can say that conduction heat from the heating surface is equal to the convection heat to the air in the cavity

$$Q_{cond.} = Q_{conv.} \quad \dots(2)$$

where

$$Q_{cond.} = -K_{eff} \cdot A_{elem.} \cdot \frac{\partial T}{\partial y} \quad \dots(3)$$

and

$$Q_{conv.} = h \cdot A_{elem.} \cdot \Delta T_O \quad \dots(4)$$

where $A_{elem.}$ is the area of the element under investigation, and,

$$\Delta T_O = T_h - T_c \quad \dots(5)$$

so that,

$$h \cdot A_{elem.} \cdot \Delta T_O = -K_{eff} \cdot A_{elem.} \cdot \frac{\partial T}{\partial y} \quad \dots(6)$$

then

$$\frac{h}{K_{eff}} = -\frac{\frac{\partial T}{\partial y}}{\Delta T_O} \quad \dots(7)$$

where $K_{eff} = K \cdot Nu$ [15], but $Nu = \frac{h \cdot H}{K}$ and H is the length of the enclosure which is the distance between the hot and cold surfaces, so that equation (6) can be written as:

$$Nu = \frac{h \cdot H}{K} = -\frac{\frac{\partial T}{\partial y} \cdot H}{\Delta T_O} \quad \dots(8)$$

4. Results and Discussion

Figs.(8) and (9) are represent photographs of the flow field at (Ri=10) and (Ri=5) respectively. These photographs show that the whole field consists of two cells which occupy all of the enclosure space, which is attributed to the fact the

fluid flow inside the enclosure is dominated by natural convection. Also it can be concluded from these photographs that, decreasing Richardson number (by increasing the Reynolds number) at constant values of Grashof number and Aspect Ratio (AR= 1), will lead to increase the force convection due to increase the amplitude of oscillation at the top wall (u_{max}). It was very difficult to image the flow field at Ri=1 and Ri=0.1, because the process requires increasing the top wall speed, which means that the time period required to complete one cycle is very little, unfortunately the facilities and the equipment for this job were unavailable at the time of experiments.

Figs. (10) and (11) represent the photographs of the flow field at (Ri=5), and various values of the Aspect Ratio (AR=0.5, and 2). It can be conclude from these figures that the time required to complete one cycle (period) will increase when the aspect ratio is increase at the same value of the Richardson number, mean that the time period is increases due to the increase the amplitude of the oscillation at the top wall (u_{max}). The temperature measurement each (1/4 and 3/4) of the time period was used to deduce experimentally the effect of Richardson number, on the average Nusselt number ($Nu_{av.}$). Fig. (12) Shows the relation between average Nusselt number with dimensionless time for different values of Richardson number (Ri=5 and 10) at constant aspect ratio (AR=1) and constant Grashof number. The figure shows that the average Nusselt number ($Nu_{av.}$) is increasing with Richardson number decrease (Ri). For example; with Ri=5 the average Nusselt number ($Nu_{av.}$) is (2.9) at ($\tau=25$), while with Ri=10 it is ($Nu_{av.}$) is (2) at the same ($\tau=25$). Also it may be concluded from the figure, that the time lag to reach the periodical steady state condition of the average Nusselt number ($Nu_{av.}$) decreases when the Richardson number decrease, for example the required time to reach the steady state condition with (Ri=10) is ($\tau=25$), while it is ($\tau=20$) with (Ri=5). The explanation of this result is that, when the Richardson number decreases the amplitude of the oscillation at the top plate (u_{max}) will increased, also the oscillation frequency of the average Nusselt number ($Nu_{av.}$) will increase which causes decrease in the time lag to reach the periodical steady state condition.

Fig.(13) shows the relation between the average Nusselt number ($Nu_{av.}$) with dimensionless time at various values of the of Aspect Ratio and constant value of Richardson number (Ri=5). It shows that the average Nusselt number is increased with increasing of the value of Aspect

Ratio at the same value of the Richardson number. For example at ($\tau = 25$), the average Nusselt number is ($Nu_{av.}=3.3$) with ($AR=2$) while ($Nu_{av.}=2.9$) with ($AR=1$), that is, the increase of the Aspect Ratio must be associated with an increase in the oscillating velocity at the top wall which causes the forced convection to increase, and will cause an improvement in the heat transfer coefficient and an increase in the average Nusselt number ($Nu_{av.}$). A comparison between the present experimental work with numerical results which was carried out by the author has been made as follows [16]:-

1. A comparison between the experimental and numerical results for the flow field is shown together in Fig.(14) for ($Ri=5$) at Aspect ratio ($AR=2$). This figure shows the effect of Richardson number and Aspect Ratio on the flow field inside the enclosure, the flow visualization photographs are given in the left column of this figure, while the numerical contour is located on the right side of the figure. Both contours of the numerical and experimental results consist of two cells and occupy all of the enclosure space. This means that the fluid flow inside the enclosure is dominated by natural convection. It can be seen from this figure that both contours have the same trend and behavior.
2. A comparison between the resulting average Nusselt number for both experimental and numerical solutions is shown in Fig's.(15) and (16). Fig.(15) shows that for ($Ri=5$) and when the steady state condition is reached at ($\tau=22$) the maximum experimental average Nusselt number ($Nu_{av.}$) was (2.9), while the maximum numerical average Nusselt number was ($Nu_{av.}=3.4$) at ($\tau=22$). Error ratio between experimental and numerical values of the

average Nusselt number in these figures is about (14.7%). Moreover Fig.(16) shows that at ($Ri=10$), and ($\tau=22$) the maximum average Nusselt number in both experimental and numerical results are ($Nu_{av.}=2$) and ($Nu_{av.}=2.3$) respectively. The error ratio between the two values is about (13%). From Fig's.(15) and (16) we may conclude that the maximum error occurs with ($Ri=5$) and minimum error occurs with ($Ri=10$), because, when the Richardson number decreases the amplitude of the oscillation at the top wall (u_{max}) will increase which causes a decrease in the time period. Also it may be concluded from these figures that the time lag to reach the periodical steady state condition of the average Nusselt number ($Nu_{av.}$) in the experimental study is greater than that for the numerical solution. For example the time to reach the steady state condition in the experimental case with $Ri=10$ is ($\tau = 20$) while in the numerical case, it is ($\tau=4$). To explain this feature: as the average Nusselt number ($Nu_{av.}$) depends on the temperature difference between the hot wall and the air inside the enclosure, and at the time just starting the experiments, the temperature of the air in the enclosure is much lower than the temperature of the hot wall, so the temperature difference between the hot wall and the air is high which will increase the heat transfer coefficient. After some time the temperature of the air will increase and cause a decrease in the temperature difference produced a decrease in the average Nusselt number continuously until reaching the steady state condition.

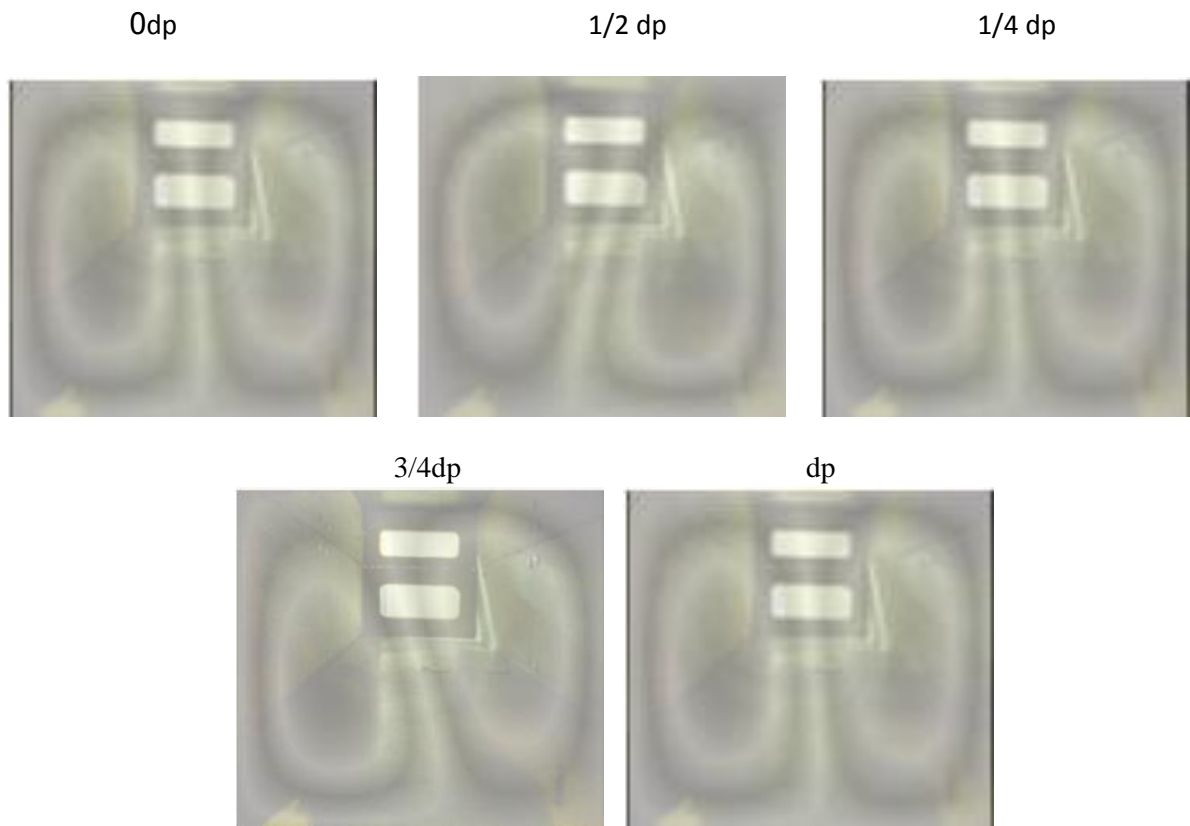


Fig. 8. Experimental flow field at $Ri=10$ and $AR=1$.

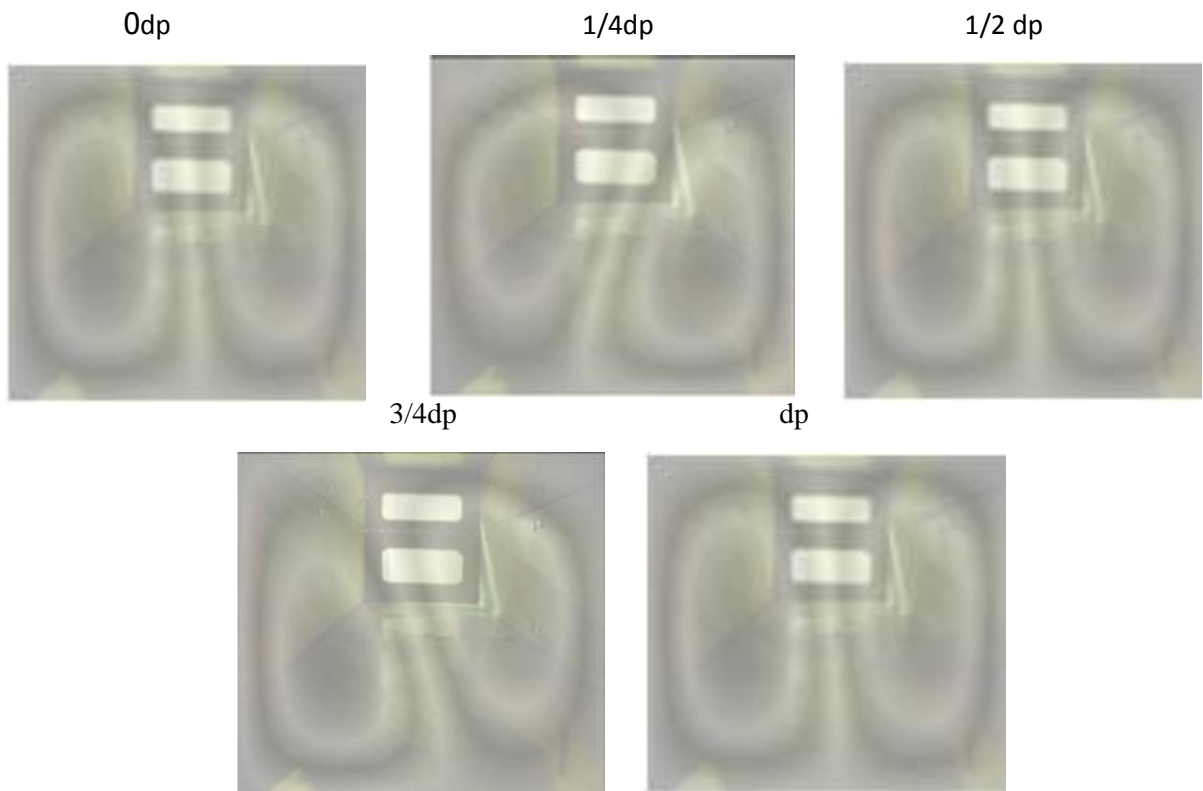


Fig. 9. Experimental flow field at $Ri=5$ and $AR=1$.

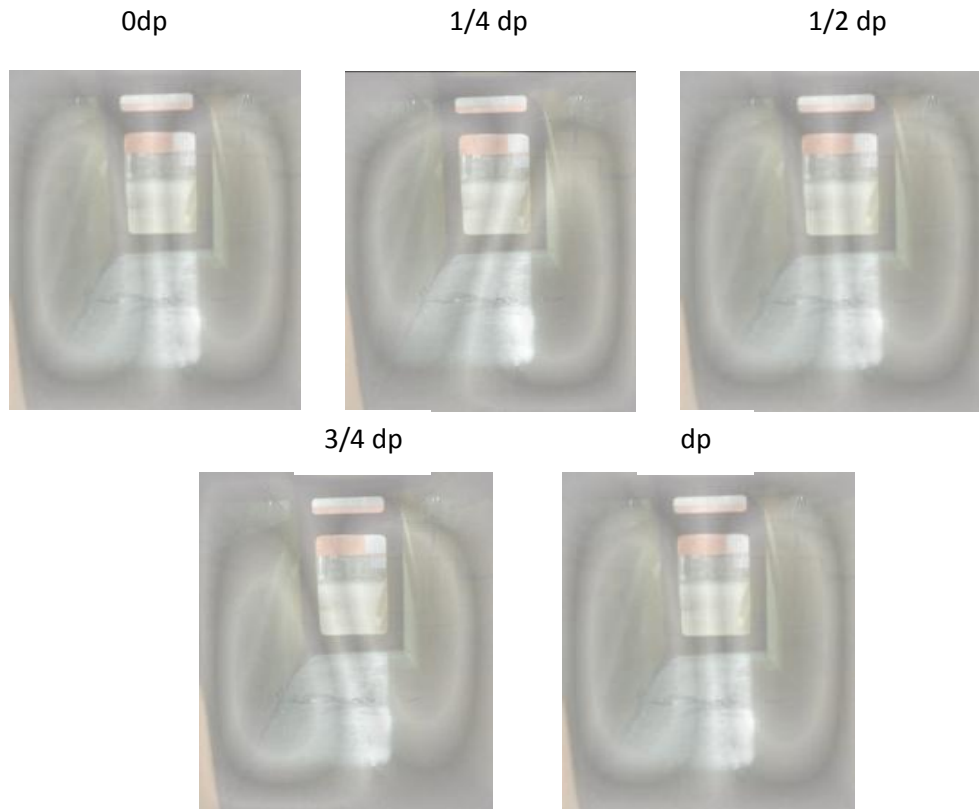


Fig. 10. Experimental flow field at $Ri=5$ and $AR=0.5$.

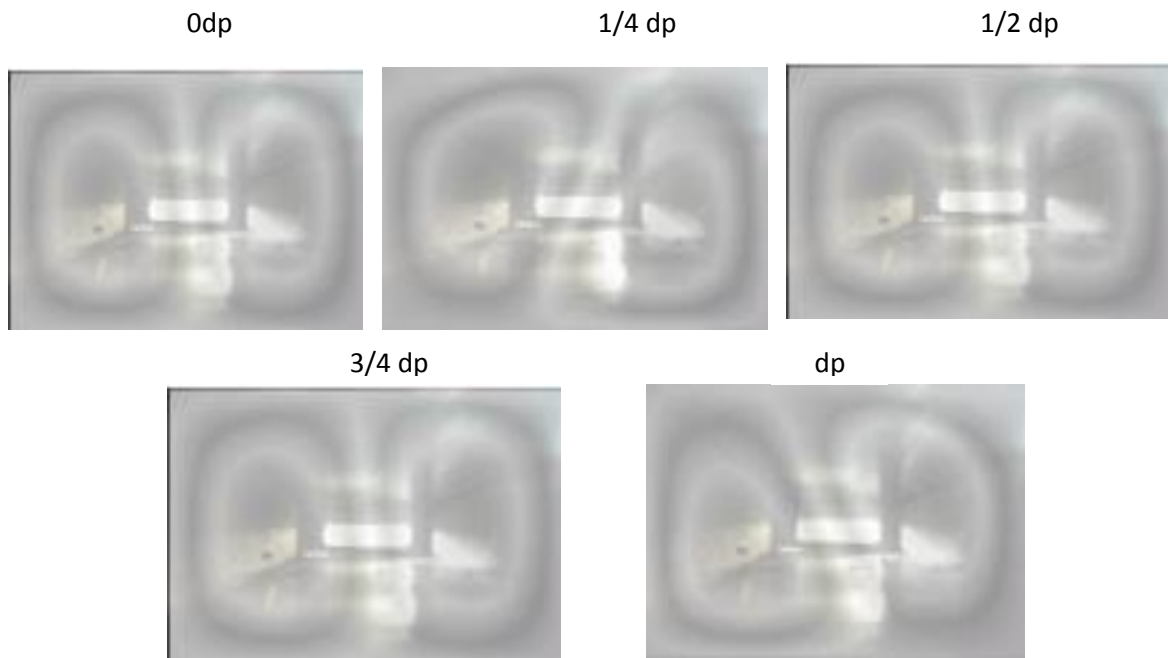


Fig. 11. Experimental flow field at $Ri=5$ and $AR=2$.

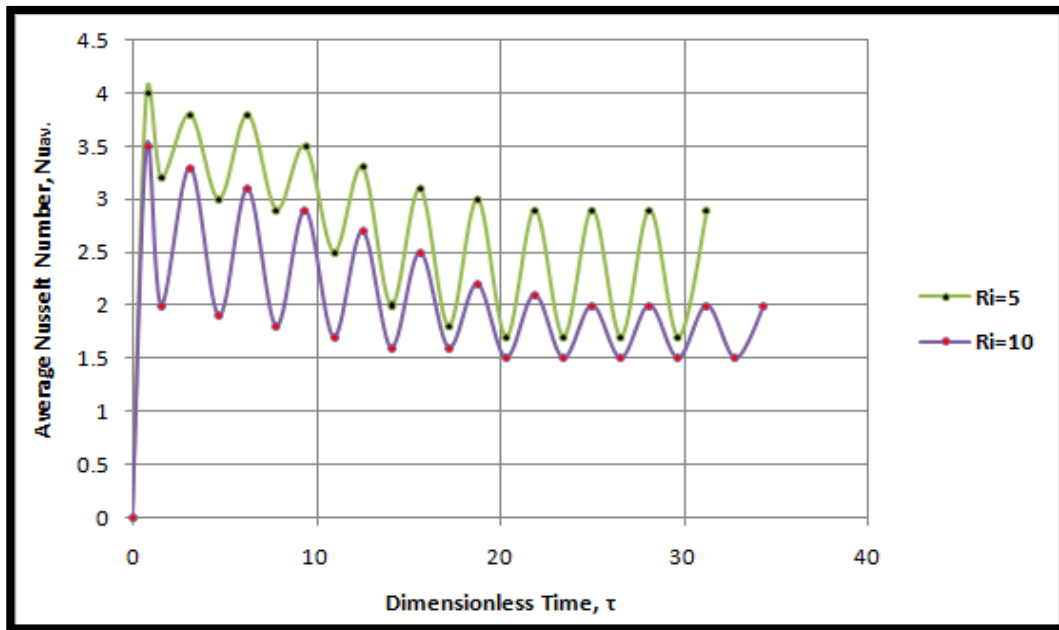


Fig. 12. Experimental determination of the average Nusselt number versus dimensionless time at Aspect Ratio(AR)= 1 with different values of (Ri) and constant (Gr).

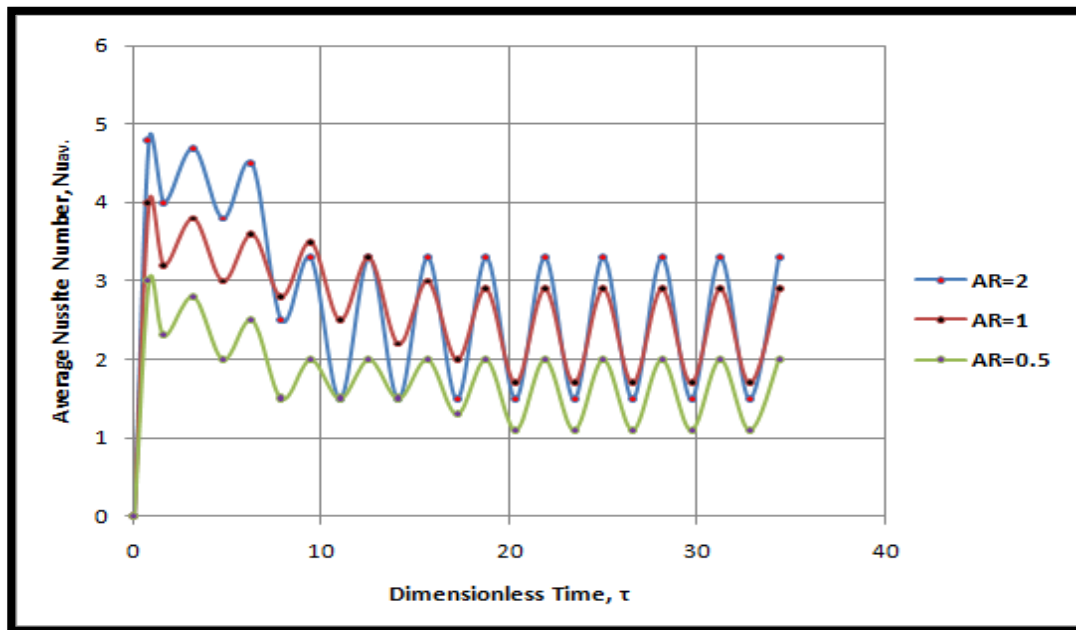


Fig. 13. The experimental determination of average Nusselt number versus dimensionless time at Richardson number (Ri=5) with different values of (AR).

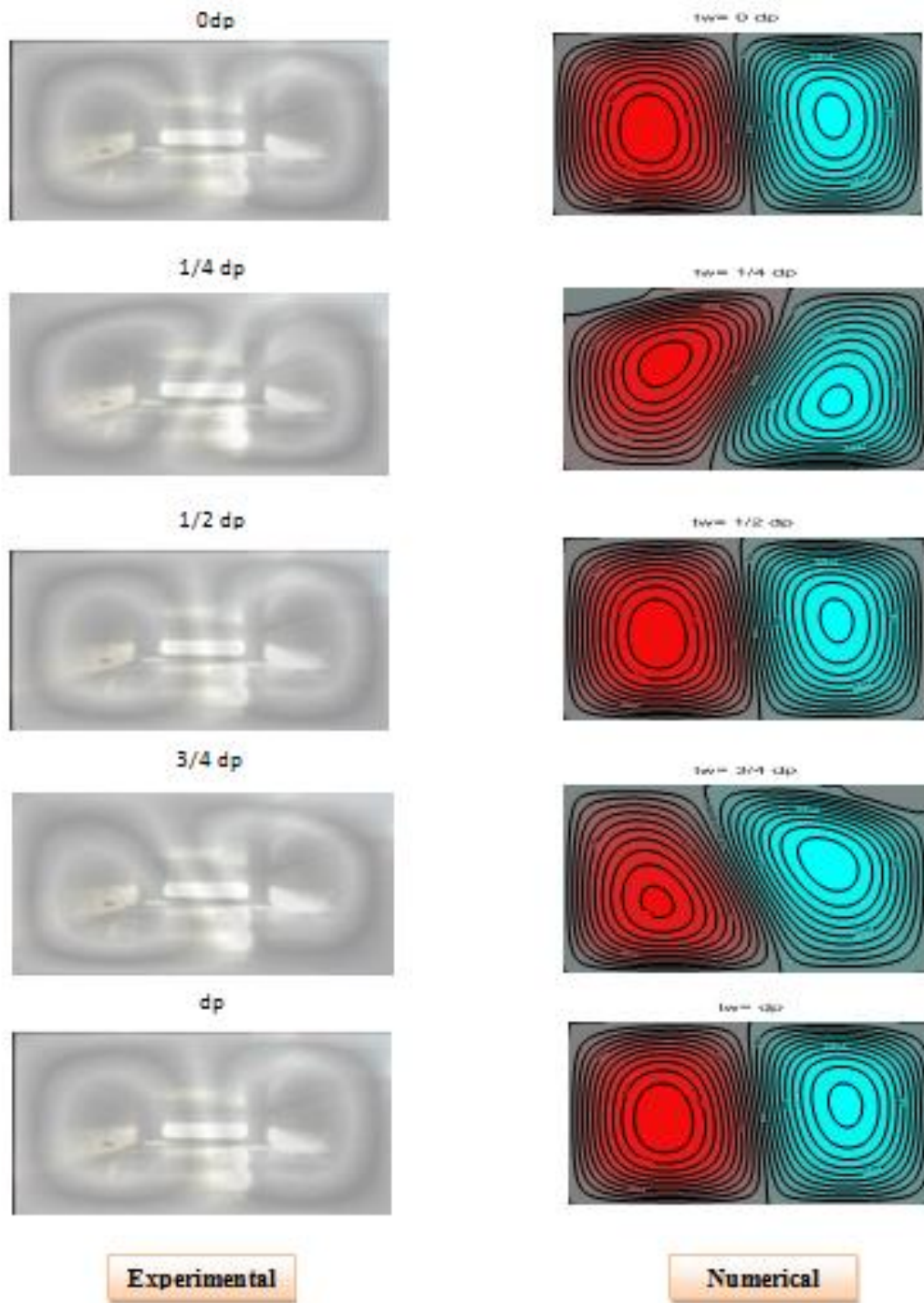


Fig. 14. Flow field, comparison of the experimental and numerical work at $Ri=5$, $AR=2$.

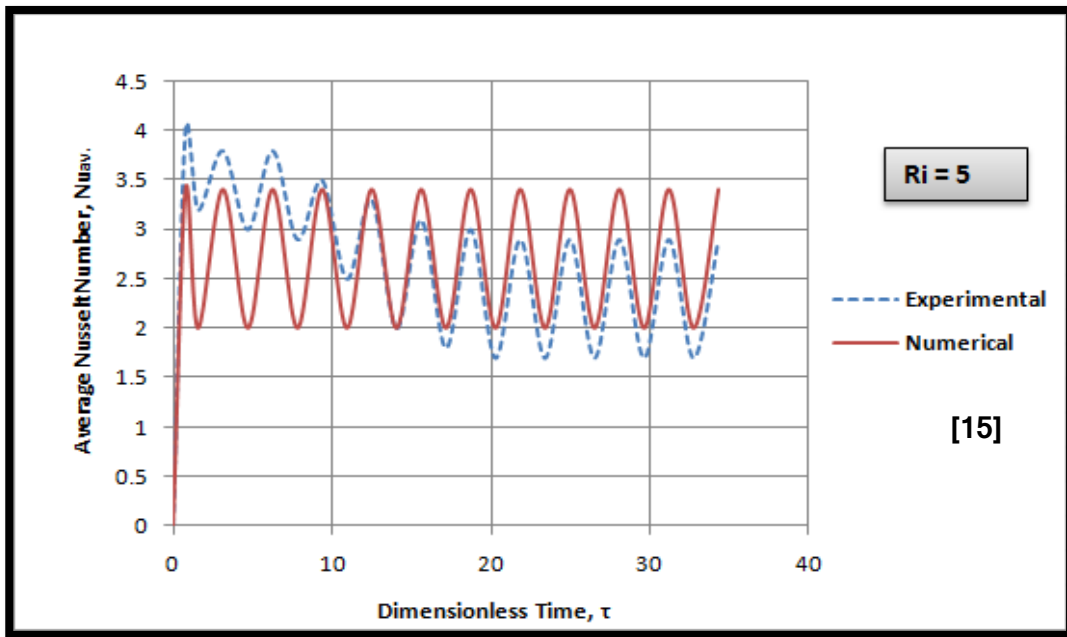


Fig. 15. Comparing the experimental and numerical work at $Ri=5$, and $AR=1$.

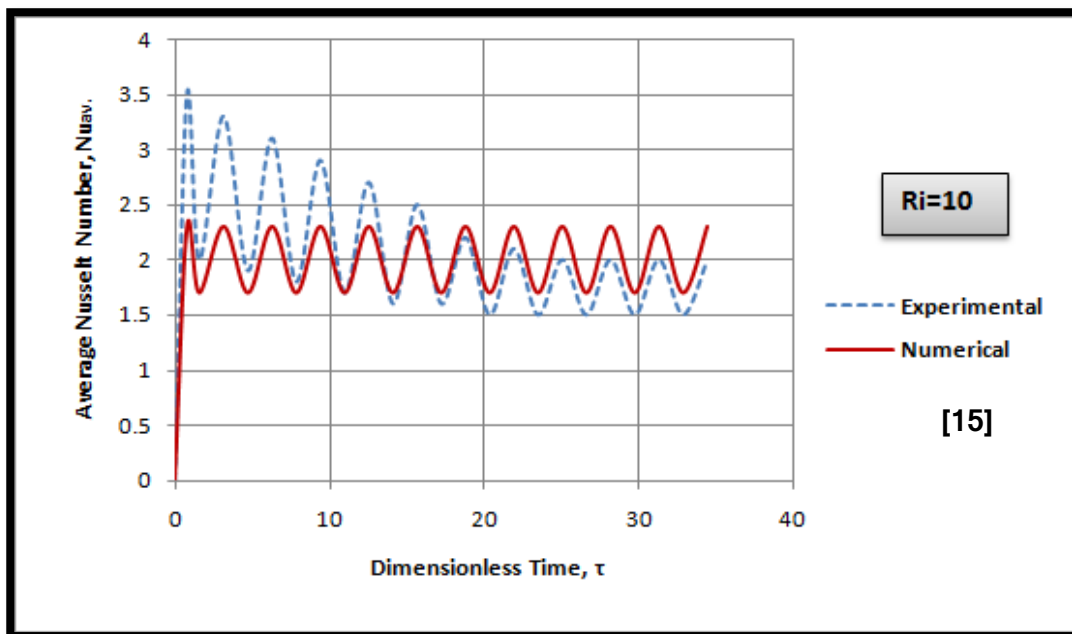


Fig. 16. Comparing the experimental and numerical work at $Ri=10$, and $AR=1$.

5. Conclusions

- 1- When Richardson number decreases due to the increase in the value of Reynolds number at constant values of Aspect Ratio and Grashof number, the time period is decrease.
- 2- The time period increases when the Aspect Ratio increases at the constant value of the Richardson number.
- 3- Average Nusselt number ($Nu_{av.}$) increases when the Aspect Ratio increases at the constant value of the Richardson number.
- 4- Time lag to reaches the periodical study state condition of the average Nusselt number ($Nu_{av.}$) decrease when the Richardson number increases.
- 5- The average Nusselt number increases when Reynolds number increases at constant values of the Aspect ratio and Grashof number.

Nomenclatures

Symbols	Definition	Units
AR	Aspect Ratio $AR=W/H$	-
A_{elem}	Area of element under investigation	m^2
dp	Dimensionless period ($dp=2\pi/S$)	-
f	Frequency	Rad
Gr	Grashof number $Gr=(g.\beta.(T_h-T_c).H^3)/\nu^2$	-
g	Acceleration due to gravity	m/s^2
H	Height of the enclosure	M
h	Heat transfer coefficient	$W/m^2.\text{ }^\circ C$
k	Fluid thermal conductivity	$W/m.\text{ }^\circ C$
Nu	Nusselt number	-
Re	Reynolds number $Re=(H.u_{max})/\nu$	-
Ri	Richardson number $Ri=Gr/Re^2$	-
r	Radius($r=15cm$)	M
S	Dimensionless frequency $S=\omega.H/u_{max}$	-
T	Dimensional value of the temperature	$^\circ C$
T_c	Cold wall temperature	$^\circ C$
T_h	Hot wall temperature	$^\circ C$
t	Time	Sec
ΔT_o	Temperature difference T_h-T_c	$^\circ C$
t_w	Dimensionless time period	-

u_{max}	Top cover speed (Amplitude of the oscillation)	m/s
Y	Dimensional length of the y-axis	M
W	Width of the enclosure	M

Greek letters

α	Thermal diffusivity	m^2/s
β	Thermal expansion coefficient	$1/^\circ k$
τ	Dimensionless time $\tau=(t.u_{max})/H$	-
ν	Kinematic viscosity	m^2/s
μ	Dynamic viscosity	$kg/m.s$
ρ	Density	kg/m^3
ω	Angular frequency $\omega=2\pi f$	rad/s

6. References

- [1] F.P. Incropera, "Convection heat transfer in electronic equipment cooling", J. Heat Transfer 110 (1988) 1097–1111.
- [2] Jae-WeonJeong, and Stanley A. Mumma, "Impact of Mixed Convection on Ceiling Radiant Cooling Panel Capacity", International Journal of HVAC&R Research, Vol. 9, No. 3, July 2003.
- [3] J.srinivasan, "Solar Pond Technology", sadhana, vol. 18, part 1,1993, pp. 39–55.
- [4] O. Aydin and W.Yang, "Mixed convection in cavities with a locally heated lower wall and moving sidewalls", Numerical Heat Transfer, Part A, 37:695 –710, (2000).
- [5] G. Guo, M. A.R. Sharif, "Mixed convection in rectangular cavities at various aspect ratios with moving isothermal sidewalls and constant flux heat source on the bottom wall", Int. J. of Heat and Mass Transfer, 43: 465–475, (2004).
- [6] H. F. Oztop, I. Dagtekin, "Mixed convection in two-sided lid-driven differentially heated square cavity", International Journal of Heat and Mass Transfer 47 :1761–1769, (2004).
- [7] A. Al-Amiri, K. Khanafer, J. Bul, I. Pop, "Effect of sinusoidal wavy bottom surface on mixed convection heat transfer in a lid-driven cavity", International Journal of Heat and Mass Transfer 50: 1771–1780, (2007).
- [8] M.A.R. Sharif, "Laminar mixed convection in shallow inclined driven cavities with hot moving lid on top and cooled from bottom", Appl. Therm. Eng. 27 :1036–1042, (2007).

- [9] M.A. Waheed, "Mixed convective heat transfer in rectangular enclosures driven by a continuously moving horizontal plate", *International Journal of Heat and Mass Transfer* 52 (2009) 5055–5063.
- [10] K.M. Khanafer, A.M. Al-Amiri, I. Pop, "Numerical simulation of unsteady mixed convection in a driven cavity, using an externally excited sliding lid" , *Eur. J. Mech. B Fluids* 26 (2007) 669–687.
- [11] Ghasemi, B., and Aminossadat, S., "Comparison of mixed Convection in a square Cavity with an Oscillating versus a Constant velocity Wall Heat Transfer", *numerical Heat transfer, Part A* , 54:726-743,(2008).
- [12] Chin-Lung Chen and Chin-Hsiang Cheng, "Experimental and numerical study of mixed convection and flow pattern in a lid-driven arc-shape cavity", *Heat Mass Transfer* (2004) 41: 58–66.
- [13] Md. N. H. Khan Chowdhury, SumonSaha and Md. A. Hassan Mamun, "Mixed convection analysis in a lid driven trapezoidal cavity with isothermal heating at bottom for various aspect anglers", *International Conference on Mechanical Engineering* 26- 28 December (2009).
- [14] J.P.Holman "Experimental Methods For Engineers "McGraw-Hill Book Company,1984
- [15] Yunus, A., "Heat Transfer: A Practical Approach", Second Edition, McGraw-Hill, (2003).
- [16] Abdull,A.S" Mixed Convection in an Enclosure with a Heated Lower Wall and Reciprocating Moving Upper Wall"M.sc thesis ,Tech.College of Baghdad 2013.

دراسة تجريبية للحمل المختلط داخل مغلف ذو سطح علوي متحرك بارد و سطح سفلي ساخن

نبيل جميل ياسين*

ضياء الدين حسين علوان**

اياد سليمان عبد الله***

*، ** قسم هندسة التبريد / الكلية التقنية الهندسية- بغداد

*** قسم هندسة التبريد / الكلية التقنية الهندسية- موصل

*البريد الالكتروني: nabiljami158@yahoo.com

**البريد الالكتروني: dhia716@yahoo.com

***البريد الالكتروني: ayad_s00@yahoo.com

الخلاصة

انتقال الحرارة بالحمل المختلط إلى الهواء داخل حيز مغلق تمت دراسته تجريبياً. ثبتت درجة حرارة السطح السفلي للحيز المغلق لتكون أعلى من درجة حرارة السطح العلوي وحرك السطح العلوي بحركة ترددية ثابتة، فيما تم عزل السطحين الجانبيين حرارياً. الفرق بدرجات الحرارة للسطحين العلوي والسفلي غيرت عدة مرات لتتم المراقبة الدقيقة للتوزيع الحراري داخل الحيز المغلق مع تغير عدد ريجاردسون. تم استخدام صندوق يمكن تغيير نسبة طولته إلى ارتفاعه كحقل اختبار لغرض تحديد تأثير عدد ريجاردسون ونسبة الطول إلى الارتفاع على شكل الحركة الهوائية داخل الحيز. تم عرض مخططات كينورمية لحركة الهواء ومعدل عدد نسلت داخل الحيز في هذا العمل. أظهرت النتائج ان معدل عدد نسلت يزداد مع نسبة الطول إلى الارتفاع بثبوت عدد ريجاردسون. كما إن نقصان عدد ريجاردسون يقلل من الفترة الزمنية بثبوت نسبة الطول إلى الارتفاع.